Pergamon

Journal of Structural Geology, Vol. 19, No. 5, pp. 621 to 637, 1997
© 1997 Elsevier Science Ltd
All rights reserved. Printed in Great Britain
PII: S0191-8141(97)00001-1
0191-8141/97 $17.00+0.00

Omphacite fabric variation in the Cabo Ortegal eclogite (NW Spain): relationships with strain symmetry during high-pressure deformation

BENITO ÁBALOS

Departamento de Geodinámica, Universidad del País Vasco, P.O.B. 644, E-48080 Bilbao, Spain

(*Received* 22 *April* 1996; *accepted in revised form* 9 *December* 1996)

Abstract—Petrostructural study of Cabo Ortegal eclogite tectonites provides an insight into the relationships between omphacite lattice-preferred orientation and the fundamental deformation parameters, in particular strain symmetry. Microstructural evidence is consistent with a tectonic origin of eclogite fabrics by coeval pyroxene plastic deformation and recrystallization under eclogite-facies metamorphic conditions. Omphacite shape fabrics and garnet spatial distributions are anisotropic and representative of the fields of either apparent flattening or constriction. Omphacite lattice-preferred orientations are dominated by [010]-axis maxima normal to the foliation (*S*-type or flattening fabrics), by [001]-axis maxima parallel to the lineation (*L*-type or constriction) or correspond to other fabric patterns described in the literature. Omphacite crystallographic fabrics are consistently asymmetric with respect to the structural framework defined by foliation and lineation. This suggests that non-coaxial deformation components (either simple or general shear) accompanied eclogite fabric development in addition to any flattening or constriction strain paths, and permit shear-sense determination. These petrostructural features were acquired in the course of eo-Hercynian ductile deformation (probably during deep subduction) under 1.5–1.7 GPa confining pressure, temperatures above 600–700°C, low differential stress (< 15–20 MPa) and slow strain rate (10^{-12}–10^{-15} s^{-1}). © 1997 Elsevier Science Ltd.

INTRODUCTION

A major challenge concerning the tectonic evolution of orogens relates to understanding the mechanisms responsible for the burial and uplift of high-pressure terrains (Schreyer, 1995), where eclogites are a common rock type. Garnet and omphacite are the major constituents of eclogites, and their chemical compositions contain fossil thermobarometric data useful for constraining their pressure–temperature evolution. Omphacite is the framework-supporting mineral in medium- and high-temperature (500–750°C, > 1.5 GPa) eclogite. Whereas garnets behave as rigid bodies, crystal-plastic processes operating in clinopyroxene enable deformation to be accommodated (Van Roermund, 1983; Godard, 1988). Hence, omphacite intracrystalline defect structures, shape fabrics and preferred lattice orientations in eclogite tectonites might be used to determine eclogite rheological properties during high-pressure metamorphism.

Slow progress in understanding the rheological behaviour of clinopyroxene-bearing rocks contrasts with current achievements in comprehending the rheology of other rock types characteristic of the crust and lithospheric mantle, such as quartzite and dunite. Results available in the literature indicate that multiple dislocation glide and/or climb, grain-boundary mobility and mass-transfer processes are the dominant deformation processes involved in plastic deformation of omphacite (Van Roermund, 1992). They control omphacite lattice-preferred orientation (LPO) development and its variations, supposed to reflect strain symmetry (Godard and Van Roermund, 1995). The postulated relationship between omphacite crystallographic fabric patterns and the strain field, in which flattening and constriction are correlated with planar (*S*-type) and linear (*L*-type) fabrics (Helmstaedt *et al.*, 1972), is impeded by the lack of knowledge on strain symmetry and the possibility of strain partitioning in eclogite-bearing tectonic units.

In contrast to knowledge of intensive thermodynamic variables, namely pressure, temperature and fluid composition (subject of much attention in the petrological, mineralogical and geochemical literature dealing with eclogites), parameters defining the kinematic framework such as stress magnitude, strain rate and finite strain are poorly known. Potentially, eclogites unaffected by retrogressive metamorphism could provide valuable information on the deformation parameters that have been operative in deeper parts of subduction and/or collision zones. However, notably due to the reasons outlined below, comparative and detailed microstructural studies devised to answer these queries are lacking in high-pressure metamorphic terrains. On the one hand, the relatively small size of eclogite bodies in several areas, as well as their frequent mode of outcrop (Eskola, 1921; Smulikowski, 1964) within strongly deformed gneiss, preclude efficient field-based eclogite structural analysis and correlation at a regional scale. On the other hand, microfabric analysis of clinopyroxene-bearing rocks is difficult and time-consuming, and before applying systematic microfabric studies to omphacite in eclogites, identification in nature and experiments of the deformation mechanisms that control the rheological behaviour of these rocks is necessary.

So far, as regards the mode of occurrence of eclogite, two likely areas suitable for integrative eclogite structural analysis at a regional scale are the (completely different from several viewpoints) eclogite-facies shear zones developed in anorthosites from the Bergen arcs of

Norway (Boundy *et al.*, 1992) and the Cabo Ortegal eclogite massif of NW Spain (Vogel, 1967; Ábalos *et al.*, 1994).

The Cabo Ortegal eclogite massif constitutes one of the largest and most continuous eclogite outcrops in the world (100–700 m thick and 17 km long). According to the classification scheme of Carswell (1990), it corresponds to a medium-temperature eclogite within tectonically thickened continental crust. The massif received the early attention of geologists from the University of Leiden, who mapped and studied it from the petrological (Vogel, 1967) and petrostructural (Engels, 1972) viewpoints. The petrostructural work of Engels (1972) on omphacite lattice-preferred orientation is one of the (if not the) most complete study of its kind ever performed (10 eclogite samples with 200 omphacite grain crystallographic orientations each), and was completed with other pioneering fabric studies on both diopside and amphibole from the eclogites and clinopyroxene from an overlying high-pressure mafic granulite. Further petrostructural attention was due to Baker and Carter (1972, one sample), in relation with seismic wave velocity and anisotropy calculation from petrofabric data, and to Godard and Van Roermund (1995). The latter authors present microfabric, transmission electron microscope (TEM) and petrostructural analyses of four eclogite samples (including one sample from Cabo Ortegal) considered as being representative of the various coaxial deformation types known so far to occur in eclogites.

The petrostructural study presented here on six Cabo Ortegal eclogite tectonites has the aim of elucidating the relationships between omphacite LPO and some of the fundamental deformation parameters (stress magnitude, strain rate and strain symmetry). Foundations of this contribution are previous field studies leading to a new structural reconstruction of the eclogite massif (Ábalos *et al.*, 1994), and an independent quantitative approximation to eclogite rheology during high-pressure metamorphism based upon the petrostructural analysis of deformed quartz veins (Ábalos *et al.*, 1996).

GEOLOGICAL SETTING

The Cabo Ortegal complex (Vogel, 1967) is a composite metamorphic nappe pile that forms a part of the so-called Allochthonous Complexes containing mafic and ultramafic rocks of the northwestern Iberian Peninsula (Arenas *et al.*, 1986). It represents a deep subduction realm active during eo-Hercynian orogeny (between 395 and 365 Ma: Peucat *et al.*, 1990; Santos Zalduegui, 1994). The complex can be divided into a basal unit with low-grade rocks, and an upper high-pressure allochthon with high-grade tectonites (Gil Ibarguchi *et al.*, 1990). The latter constitutes a composite nappe pile displaying inverted metamorphism and containing a basal, migmatitic, high-pressure gneiss, and mafic (eclogite and granulite) and ultramafic (metaperidotite) high-pressure rocks on top. The eclogite massif studied here crops out between the gneiss and the high-pressure granulite along the eastern part of the Cabo Ortegal complex (Fig. 1).

STRUCTURE AND COMPOSITION OF THE ECLOGITE MASSIF

On the basis of its isotopic and geochemical signatures (Bernard-Griffiths *et al.*, 1985), the Cabo Ortegal eclogite massif is inferred to constitute a piece of destroyed Palaeozoic oceanic lithosphere. Petrographically, eclogites are medium- and fine-grained, and primarily composed of garnet, omphacite, quartz, zoisite and rutile. Garnet and omphacite constitute 90–95% of the total mineral content. Detailed petrographic descriptions of these rocks were given by Vogel (1967) and Gil Ibarguchi *et al.* (1990). Field structural and petrographic criteria permit the 100–700 m thick and 17 km long eclogite outcrop of Cabo Ortegal to be considered as being composed of two principal eclogite types each with its own cartographic distribution (Fig. 1). Although both eclogite types exhibit penetrative foliations which represent deformations, based on their field appearance they are described here, following Ábalos *et al.* (1994), as (1) massive eclogite and (2) deformed (mylonitic, although under eclogite-facies conditions) eclogite in shear zones.

The 'massive eclogite' contains the garnet–omphacite ($\pm$quartz, rutile and zoisite) mineral assemblage. It recrystallized under *ca* 800°C and >1.7 GPa (Gil Ibarguchi *et al.*, 1987, 1990) and exhibits a tectonic fabric related to a D_1 high-pressure tectonothermal event. The 'deformed eclogite' crops out in ductile shear zones that at a map scale bound larger slices (*ca* 100 m thick and 5–10 km long) of the 'massive eclogite'. It, too, contains the garnet–omphacite ($\pm$quartz, rutile and zoisite) mineral assemblage, but recrystallized at *ca* 600–800°C and >1.3–1.7 GPa (Gil Ibarguchi *et al.*, 1990). The tectonic fabric these rocks exhibit has been interpreted as due to high-temperature mylonitization of the 'massive eclogite' related to eclogite slice stacking during a high-pressure D_2 deformation phase.

The 'massive eclogite' slices and the bounding shear zones with 'deformed eclogite' dip moderately to the WNW (Fig. 2) and exhibit the geometry of an antiformal duplex stack (Fig. 3). Although mineral lineations tend to plot as a dispersed distribution within the foliation, they exhibit a preferred orientation plunging to the NNE (Fig. 2) and are associated with a NNE-directed sense of movement of hangingwall blocks (relative to present-day geographical co-ordinates). These directions coincide with those developed under similar metamorphic conditions in the metaperidotite, high-pressure granulite and in the high-pressure gneiss (Fig. 3) that over- and underlie the eclogite (Girardeau *et al.*, 1989; Ábalos *et al.*, 1994).

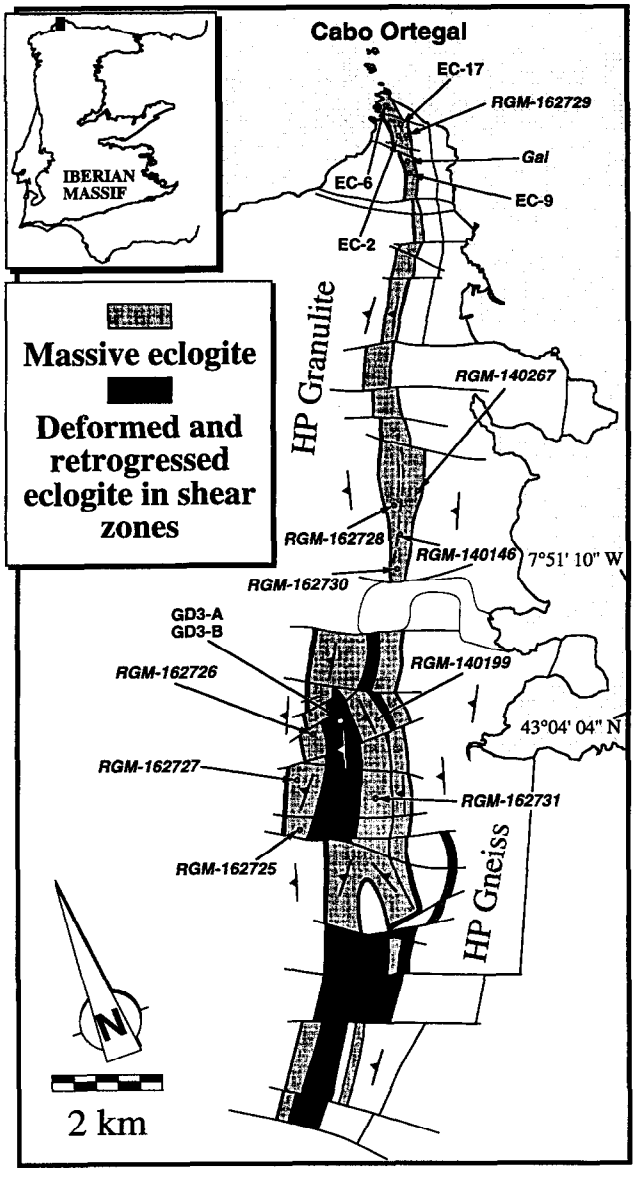

Fig. 1. Geological map of the Cabo Ortegal eclogite outcrop showing the location of the samples collected for omphacite lattice-preferred orientation measurement in this study (samples EC and GD3), together with the location of the samples studied by Engels (1972, samples labelled RGM) and by Godard and Van Roermund (1995, sample Gal).

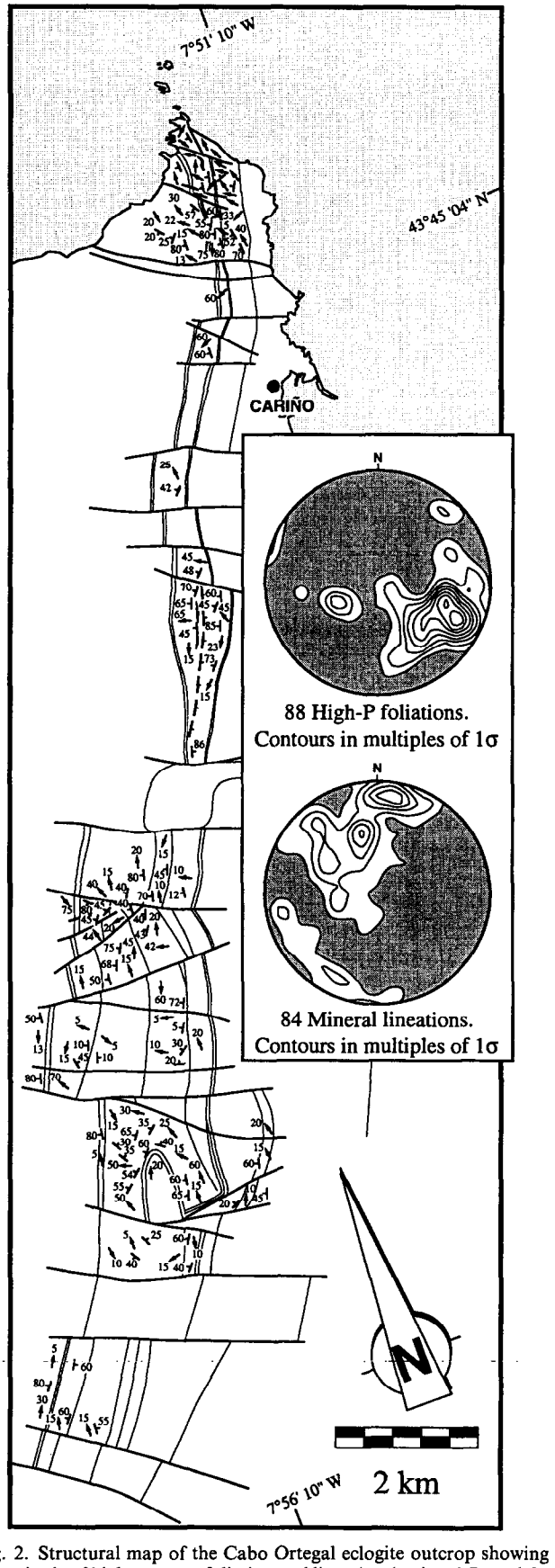

Fig. 2. Structural map of the Cabo Ortegal eclogite outcrop showing the attitude of high-pressure foliation and lineation (regional D_1 and D_2 structures) and the respective equal-area stereoplots. Note that geographic north on the map is oblique to the geographic north on the stereoplots.

ECLOGITE FOLIATION/LINEATION AND SAMPLE DESCRIPTION

Massive eclogite

The massive eclogite exhibits a penetrative continuous foliation defined by variations in the relative proportion of the mineral constituents and by omphacite shape-preferred orientation. A weak mineral lineation is defined on the foliation planes by zoisite, quartz and omphacite shape-preferred orientation (Figs 4 and 5).

Garnets form slightly subhedral crystals of 1–2 mm (Fig. 4b) and up to 4 mm (Fig. 4a, c & d) in diameter with rather homogeneous compositions (Gil Ibarguchi *et al.*, 1990). Ábalos *et al.* (1995) found statistically uniform but

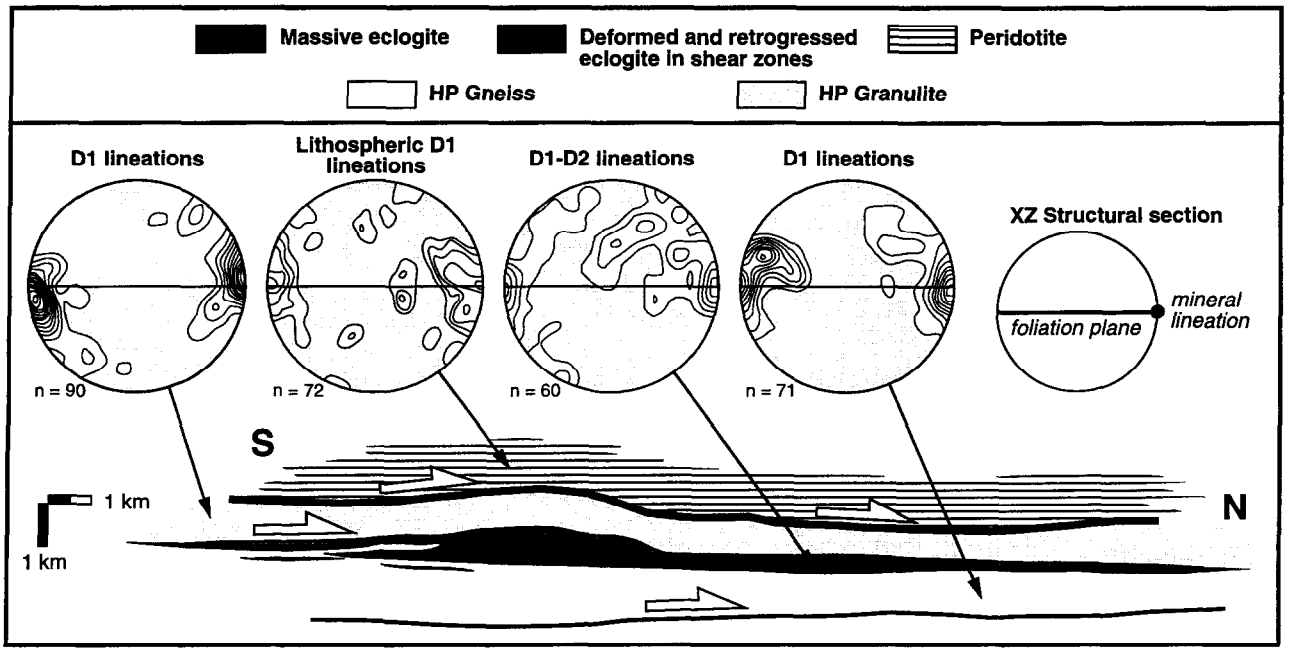

Fig. 3. Reconstructed cross-section of the upper allochthon of Cabo Ortegal. The plane of projection trends N20°E, dips 40° to the ESE, and is both parallel to the regional lineation and perpendicular to the foliation. Stereoplots show D_1–D_2 lineation data for the different lithotectonic units involved and have been conveniently rotated to fit the down-dip structural section. Lower-hemisphere, equal-area projections. Contours in multiples of uniform distribution.

anisotropic garnet spatial distributions in these rocks, describable through a triaxial ellipsoid with normalized $X{:}Y{:}Z$ ratios of 1.28:1.00:0.84. Flinn's k parameter for this ellipsoid has a value of 1.473 (Flinn, 1962).

Elongated clinopyroxene grains (1000–2000 × 300–500 μm in size) often occur in polycrystalline domains forming the eclogite framework (Figs 4c, d & 5a). In oriented structural XZ and XY sections (XY, plane of foliation; X, mineral lineation direction) these exhibit shape fabrics with long to short axis ratios of 2–4 (Table 1) and are clearly oriented parallel to the mesoscopic foliation (Figs 4c & 5a). This orientation is also recognizable in hand specimen and at the outcrop scale. The primary clinopyroxenes are omphacite with *ca* 30–35 mol% of jadeite and a generally low acmite content (0–4 mol%). Solid-state plastic deformation of omphacite is deduced from slight undulatory extinction and subgrain occurrence. Secondary, symplectitic, pyroxenes appear complexly intergrown with sodic plagioclase, but retain their parent crystallographic orientation so efficiently that recognition of the original boundaries of the oriented primary clinopyroxenes is still possible (Fig. 4e). The symplectites after omphacite exhibit TEM microstructures indicating that omphacite deformation pre-dated symplectite formation (Godard and Van Roermund, 1995). Omphacite spatial distribution was found to be statistically homogeneous and anisotropic (Ábalos *et al.*, 1995), being describable with a triaxial ellipsoid with normalized $X{:}Y{:}Z$ ratios of 1.40:1.00:0.76 for which the Flinn's k parameter has a value of 1.06. All this evidence is consistent with a tectonic origin of the eclogite fabrics by coeval pyroxene plastic deformation and metamorphic recrystallization (Buatier *et al.*, 1991).

Amphiboles have pargasitic to Mg-hornblende compositions. They are commonly the products of clinopyroxene retrogression. LPOs of omphacite and secondary hornblende from eclogite sample RGM162727 measured by Engels (1972) demonstrate that hornblende orientation (the point maximum for [001] in the amphibole coincides with the point maximum for [001] in the clinopyroxene) is determined by the orientation of pre-existing omphacite and that, most likely, this mineral grew homotaxialy at the expense of omphacite.

Four massive eclogite samples (EC2, EC6, EC9 and EC17) were selected for crystallographic fabric measurement on the basis of their manifest deformational features (from the viewpoints of both field, meso- and microstructures), almost absent retrogression and differences in grain size (Figs 4 and 5). Whereas samples EC2, EC6 and EC9 are petrographically similar, EC2 (Fig. 4a) contains coarser garnets (up to 2 mm) and omphacites (1000 μm on average), and EC6 (Fig. 4b) finer-grained (< 1.2 mm) garnets and *ca* 548 μm omphacite (Table 1). All of the samples were collected from the basal slice of the Cabo Ortegal eclogite duplex stack (Fig. 1). Fabrics from other samples of this slice were studied by Engels (1972, five samples) and Godard and Van Roermund (1995, one sample), and the former also measured fabrics from samples of the second (two samples) and third (three samples) slices (Fig. 1). Omphacite grain size and shape fabrics were measured directly in the micrographs of Figs 4 and 5, and provide the values of the XZ, YZ and XY ratios presented in Table 1. The values of Flinn's

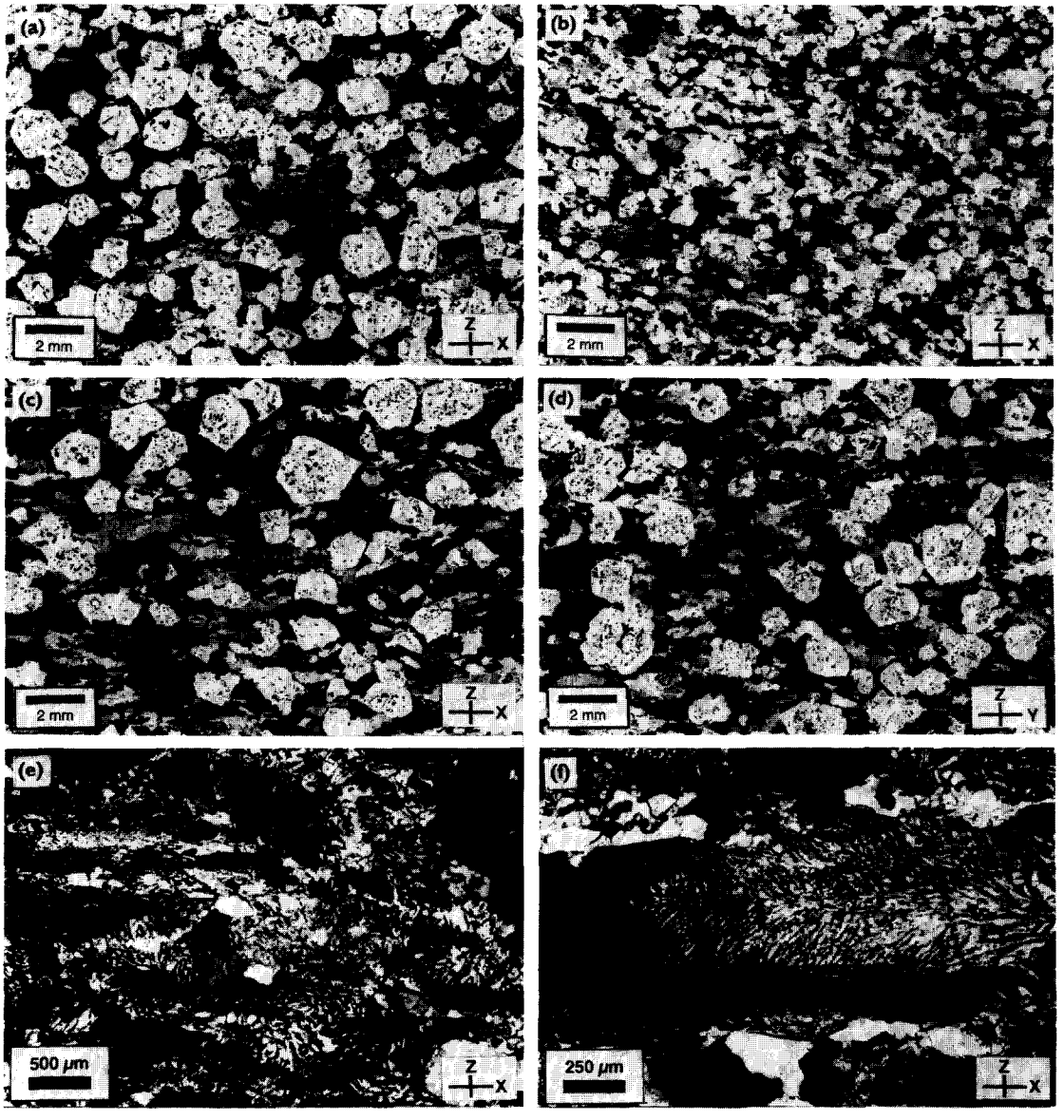

Fig. 4. Optical micrographs of deformational microstructures from Cabo Ortegal eclogite samples deformed during regional D_1. (a) Sample EC2 (*XZ* structural section). (b) Sample EC6 (*XZ* section). (c) Sample EC9 (*XZ* section). (d) Sample EC9 (*YZ* section). These four micrographs were taken under crossed nicols and are presented here as negative images, thereby garnets appearing in white and light grey. Note the differences in garnet and omphacite grain size. (e) and (f) Conventional positive optical micrographs under crossed polars showing local microstructures from sample EC9 due to omphacite symplectitization. Note that the boundaries of the original omphacites and its shape-preferred orientation are still recognizable in spite of the clinopyroxene being completely retrogressed to a plagioclase–clinopyroxene aggregate.

(1962) k parameter calculated for them are of the order of 0.89–1.06 (this study) and 0.4 (Godard and Van Roermund, 1995), and plot primarily in the field of apparent flattening. Sample EC17 (Fig. 5a–d) is petrographically somewhat different to the others, in spite of its similar mineral chemistry. This eclogite contains both kyanite and phengite, and exhibits polycrystalline omphacite aggregates elongated parallel to the mineral lineation. X:Y:Z dimensions for these aggregates are usually in the range > 100–70:40–30:8–5 mm. Respective shape ratios average 3 on the foliation plane (*XY* sections; Fig. 5c), > 10 in *XZ* sections (Fig. 5a) and 1–3 in *YZ* sections (Fig. 5b). The elongated nature of these aggregates (Fig. 5d), together with the geometrical relationships of mineral lineations and the calculated value of Flinn's k parameter of 0.9–2.9, all appear to indicate that these represent a stretching lineation formed under apparent constriction.

Deformed eclogite

The penetrative structures associated with the deformed eclogite are, at the outcrop scale, a continuous foliation, and mineral and stretching lineations. From the microstructural point of view, omphacite grain-size reduction (283–345 μm, Table 1) and shape/crystallo-

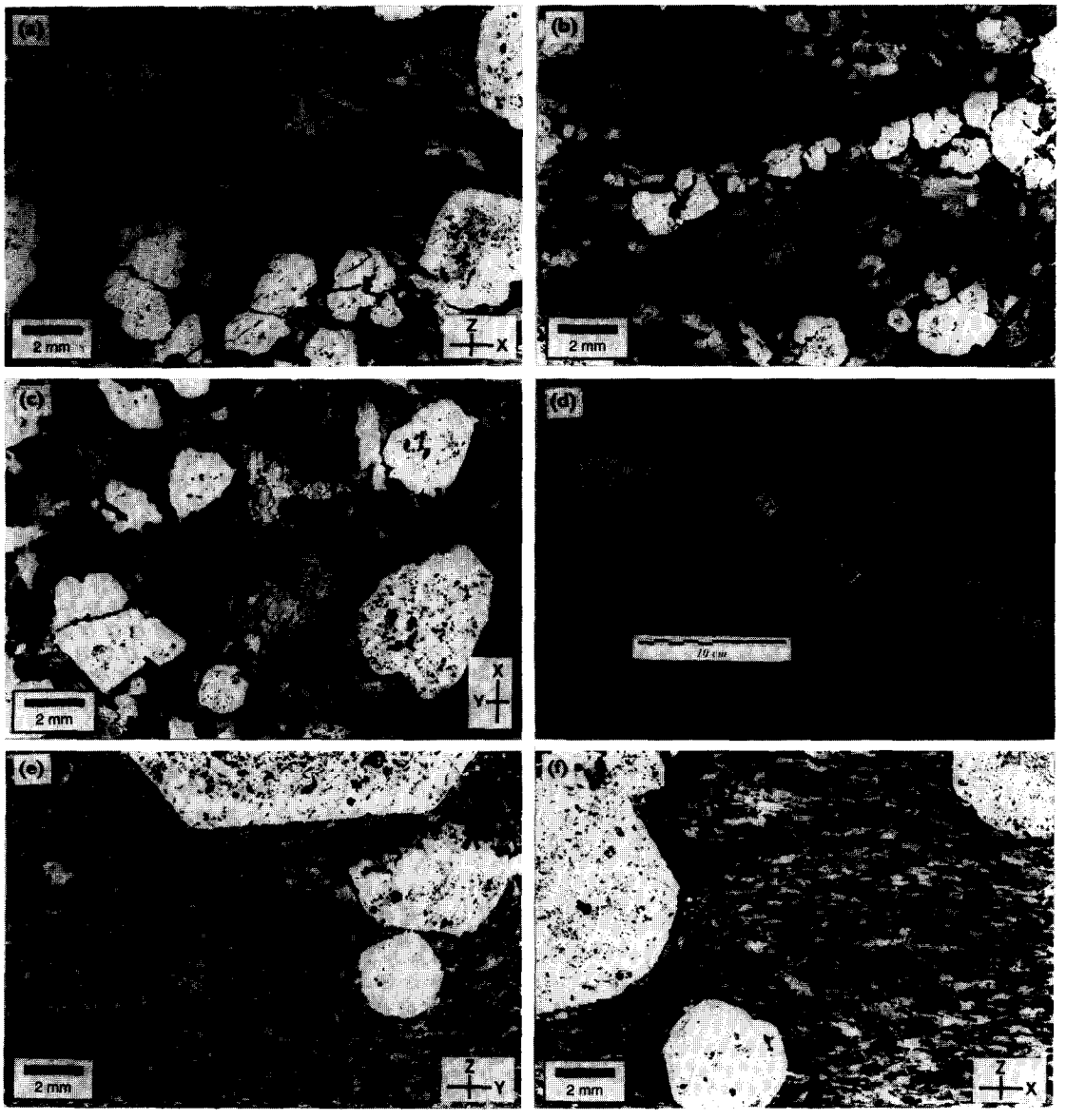

Fig. 5. Optical micrographs of deformational microstructures from Cabo Ortegal eclogite samples deformed during regional D_1 (sample EC17) and D_2 (samples GD3). (a) Sample EC17 (XZ structural section). (b) Sample EC17 (YZ section). (c) Sample EC17 (XY section). (d) Hand specimen of sample EC17 cut along the foliation (XY section) to show mesoscopic features of lineation (arrow in the X direction). (e) Sample GD3A (YZ section). (f) Sample GD3B (XZ section). Micrographs (a), (b), (c), (e) and (f) were taken under crossed nicols and are presented here as negative images. Note the remarkable differences in garnet and omphacite grain size and microstructure between the 'massive eclogite' (sample EC17 and micrographs from Fig. 4) and the 'deformed eclogite' (samples GD3).

graphic-preferred orientation, as well as impressive growth of cm-sized (> 1.5 cm) garnet porphyroblasts, are conspicuous (Fig. 5e & f). Garnet spatial distribution in these eclogites is also statistically homogeneous and anisotropic, and the corresponding triaxial ellipsoid has normalized X:Y:Z ratios of 1.33:1.00:0.80, and a Flinn's k parameter (Flinn, 1962) of 1.32, representative of the field of apparent constriction (Ábalos *et al.*, 1995). Omphacite shape fabrics exhibit X:Y:Z ratios of 2.00:1.00:0.50 and k parameters of *ca* 1. Garnet and clinopyroxene composition in these rocks are not very different from those of the massive eclogite (Gil Ibarguchi *et al.*, 1990).

Two deformed eclogite samples, GD3A (Fig. 5e) and GD3B (Fig. 5f), were selected for crystallographic fabric measurement and microstructural study. According to the revised eclogite outcrop delineation and structural interpretation of Ábalos *et al.* (1994), these rocks define high-pressure and high-temperature shear zones (up to 200 m thick) with highly deformed eclogite that bounds lens-shaped slices of the massive eclogite (Figs 1 and 2). No previous clinopyroxene fabric study has been published on these rocks, described as the so-called "Doubtful Paragneisses" by Vogel (1967) and Engels (1972). Both authors proposed a relationship (in spite of their rather different petrographical and compositional fea-

Table 1. Garnet and omphacite grain size and shape fabrics

Sample	Section	Grain size (μm)		Omphacite shape fabric		
		Garnet	Omphacite	Long axis (mm)	Short axis (mm)	Shape ratio
EC2	*XZ*	<2000	1000	<2.0	<0.5	4.0
EC6	*XZ*	<1200	548	1.0	0.3	3.3
EC9	*XZ*	<2500	642	0.9	0.3	3.0
	YZ	<2500	642	0.6	0.3	2.0
EC17	*XZ*	<4300	1113	<4.7	<0.4	<15.0
	YZ	<4300	1113	1.3	0.4	3.2
	XY	<4300	1113	3.8	3.1	1.3
GD3A	*YZ*	<15,000	283	0.4	0.2	2.0
GD3B	*XZ*	<15,000	345	0.6	0.2	3.0

tures) between the 'deformed eclogite' described here and the pelitic paragneiss formation underlying the Cabo Ortegal eclogite.

OMPHACITE FABRIC MEASUREMENT

In view of the contrasting structural position, microstructures and tectonic meaning of the six samples described above, U-stage measurements of omphacite crystallographic axes were made with the aim of obtaining a general insight into the orientation of clinopyroxene and to provide further constraint on the kinematic history (whether the preferred orientation could be correlated with megascopic structures of distinct deformation events) and deformation mechanisms. Oriented thin sections were cut parallel to principal structural sections, *XY*, *XZ* or *YZ*. Orientations of the axes of the optical indicatrix α, β and γ, and one {110} cleavage plane, were determined directly on a five-axis Leitz universal stage. From these orientations, the [001] (*c*-axis), [010] (*b*-axis) crystallographic directions and π(100) (the pole to (100) omphacite planes) were constructed using stereographic procedures by plotting the intersections of the {110} cleavages with the optic plane normal to β. One hundred and twenty-five measurements of the aforementioned optical and crystallographic axes were made and calculated for each sample.

Unravelling omphacite LPO asymmetry with respect to external foliation and lineation, which might also be used to show evidence of rotational deformation components and shear-sense determination, requires careful sample thin section preparation and crystallographic data representation. In the fabric stereoplots presented in Fig. 6 (contoured in multiples of uniform distribution) the projection planes always correspond to structural *XZ* sections (*XY*, foliation; *X*, lineation direction). Fabrics measured in sections other than *XZ* (e.g. GD3A) were conveniently rotated for graphic presentation. The foliation plots as the equatorial diameter (vertical E–W), whereas the lineation is horizontal within this plane. The horizontal lines across the stereoplots delineate the trace of macroscopic foliation, whereas lineation is located at its intersection with the stereoplot's outer great circle. This mode of fabric data presentation is the conventional one used in the literature for most mineral fabric studies (e.g. for quartz and olivine) and was followed here to facilitate recognition of the geometrical relationships between LPOs and the structural *XYZ* framework.

Reference frames commonly used for omphacite fabrics in the literature include those that use orientation of general sections, with respect to either internal sample or geographical co-ordinates, as projection planes (e.g. Engels, 1972), and others that employ projection planes related to geographical co-ordinates and attitude of foliation and lineation (e.g. Boundy *et al.*, 1992). For example, if foliation planes were visible in the hand specimen, omphacite LPOs in eclogite general sections were also represented as great circles on the stereoplots by Engels (1972). Otherwise, the position of the best-fit great circle (normal to one fabric eigenvector and containing the other two) was plotted so as to enhance single point-maxima or girdle fabric distributions (Fig. 7). In all of these situations crystallographic fabrics are roughly symmetrically arranged with respect to foliation and lineation, and this has led to interpretation (Van Roermund, 1992; Godard and Van Roermund, 1995) that they formed mostly under coaxial deformation regimes.

OMPHACITE FABRICS

The categorization of omphacite fabrics in pattern types can be misleading as intermediate patterns exist and a variety of other features cannot be simply categorized, although others have tried to previously. In order to allow these complex variations to be tabulated and to show the geometrical relationships between the crystallographic fabrics and the external *XYZ* structural framework, the eigenvectors and eigenvalues were calculated for each of the [001], [010] and π(100) omphacite LPOs measured.

Eclogite fabric description and classification

For the description of the clinopyroxene fabrics

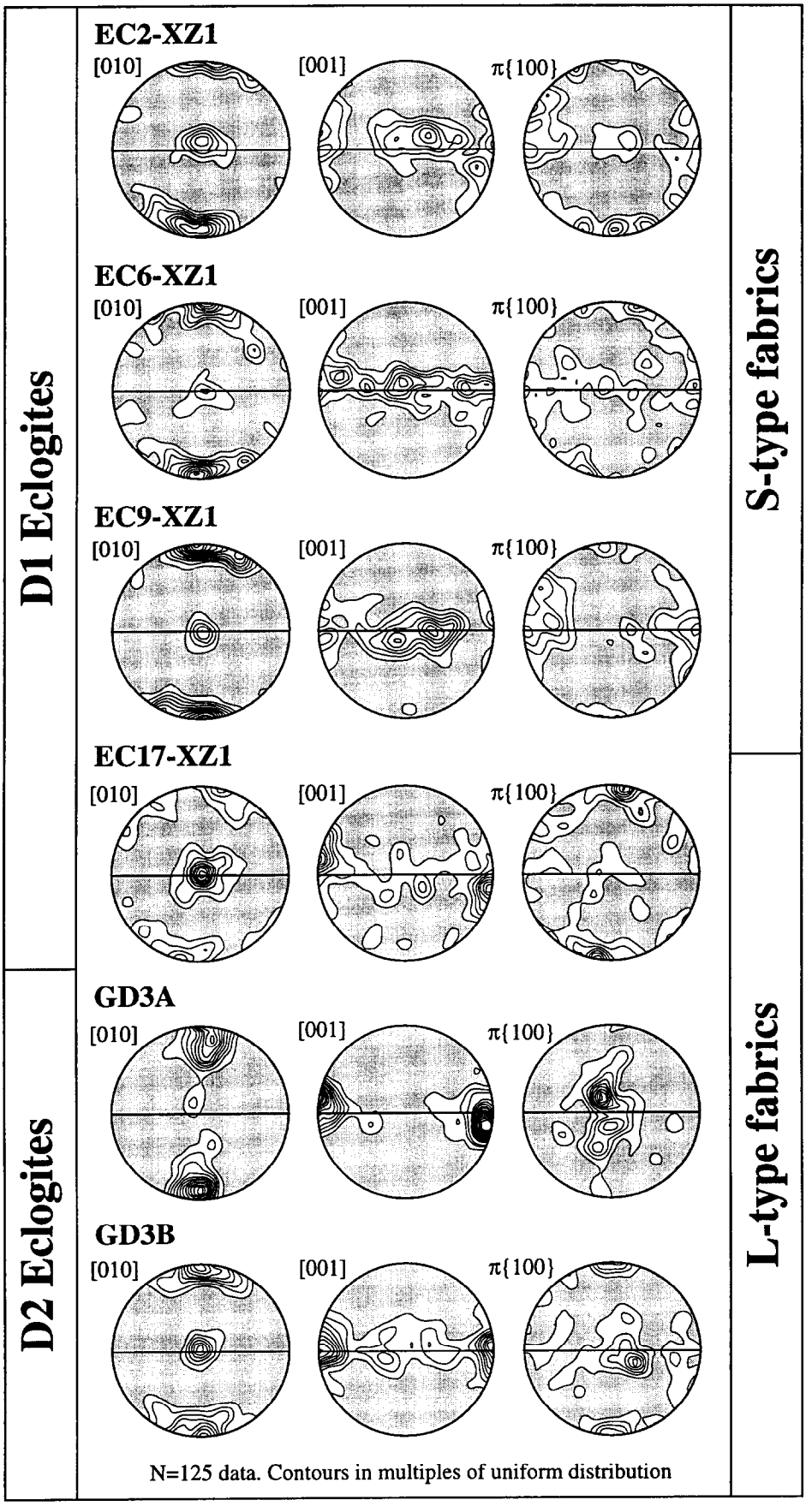

Fig. 6. Omphacite lattice-preferred orientation stereoplots (lower-hemisphere, equal-area projections) for the six eclogite samples studied. See text for further details.

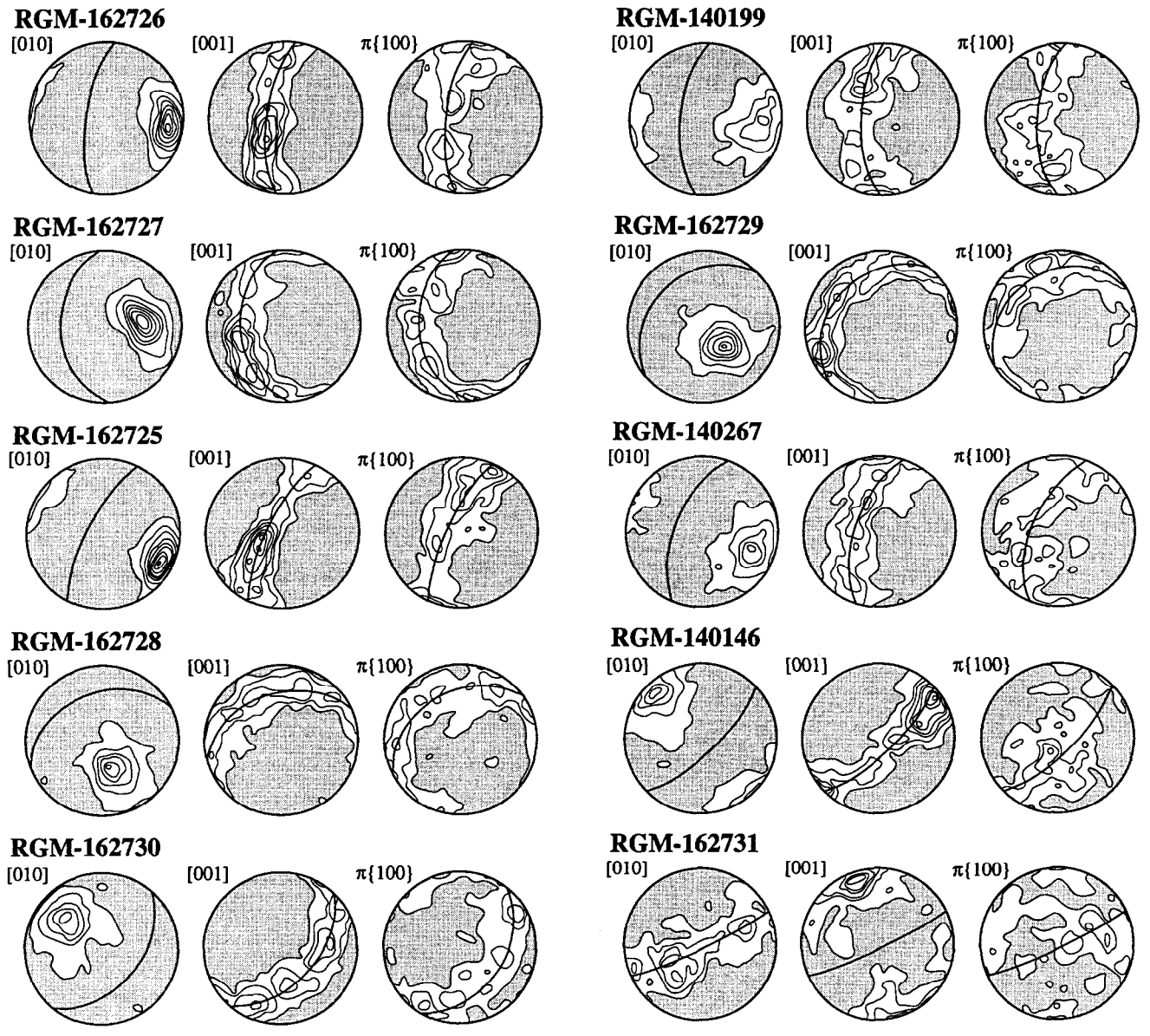

Fig. 7. Omphacite lattice-preferred orientation stereoplots (lower-hemisphere, equal-area projections) for the eclogite samples studied by Engels (1972). Two hundred measurements in each sample. Contour intervals: 1%.

measured in this study (Fig. 6), a refined version, since applied exclusively to eclogites, of the classification proposed by Godard and Van Roermund (1995) is used. This new approach is based on a survey of the literature of omphacite fabrics including the outstanding, intuitive and successful classification of Helmstaedt *et al.* (1972), here considered as a benchmark in eclogite fabric studies, and the LPOs of pyroxenite layers in ultramafic complexes now known also to occur in eclogites. The patterns of omphacite-preferred orientation that emerge from this scheme are, in order of their frequency of occurrence in the literature on eclogites, as follows.

Pattern 1, 'S-type or flattening fabrics'. These exhibit crystallographic [010]-axes concentrated on a maximum normal to the foliation, whereas [001] is dispersed into a great circle perpendicular to [010]. Eclogite specimens of this group show a well-defined foliation, and this fabric type was referred to as *S*-type by Helmstaedt *et al.* (1972). Nine of the Cabo Ortegal eclogite's omphacite LPOs measured by Engels (1972) (Fig. 7), the one measured by Godard and Van Roermund (1995) (Fig. 8) and the omphacite fabrics from samples EC2, EC6 and EC9 in this study (Fig. 6) belong to this group. However, on the basis of the orientation of [001] submaxima inside the [001] girdle, fabric variations arise with [001] submaxima parallel and/or normal to the mesoscopic lineation (Fig. 6). Boundy *et al.* (1992) found [001] girdles with submaxima parallel to the mineral and stretching lineation in eclogites after anorthosite within shear zones. Other fabrics of this type have been reported in the literature by Yoshino (1961, 1964), Banno and

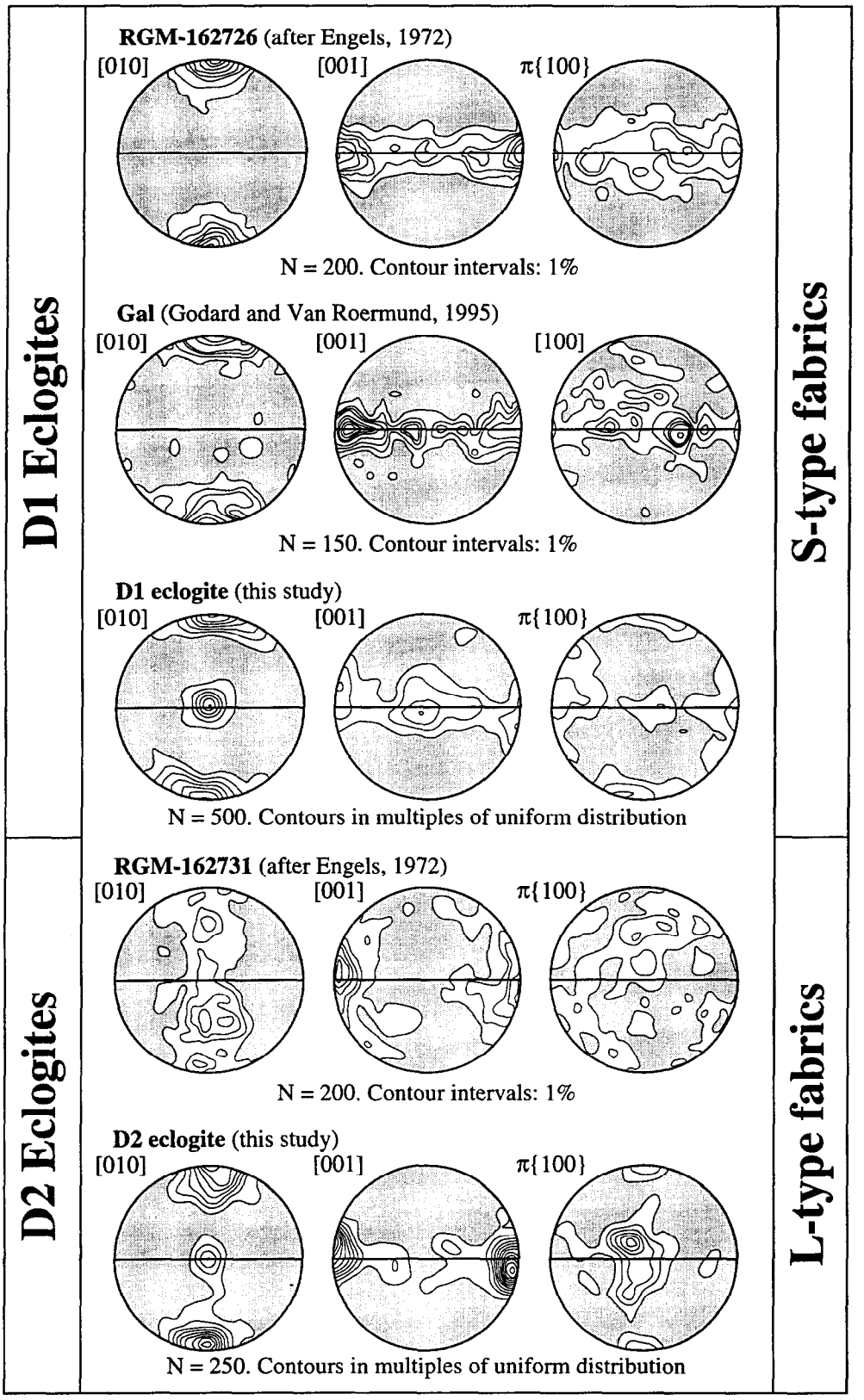

Fig. 8. Omphacite lattice-preferred orientation stereoplots selected to show the close correspondence between *S*-type omphacite fabrics and the 'massive eclogite' (deformed during high-pressure D_1, and thus labelled 'D_1 eclogites') and between *L*-type omphacite fabrics and the 'deformed eclogite' (deformed during high-pressure D_2, and thus labelled 'D_2 eclogites' in the figure). The fabric labelled 'D_1 eclogite' was obtained by plotting together the crystallographic axis orientations of samples EC-2, EC-6, EC-9 and EC-17 (500 grains). Accordingly, the fabric labelled 'D_2 eclogite' was obtained by plotting together the crystallographic axis orientations of samples GD3A and GD3B (250 grains). Fabrics RGM-162726 and RGM-162731 after Engels (1972, see also the original fabrics in Fig. 7) were rotated assuming that the [001] maxima was parallel to the lineation and redrawn in the structural reference framework used for the other diagrams. Lower-hemisphere, equal-area projections.

Yoshino (1965), Kozlowski (1965), Kumazawa *et al.* (1971) and Godard and Van Roermund (1995).

Pattern 2, 'L-type or constriction fabrics'. These contain a relatively strong [001]-axis maximum parallel to a commonly pronounced mesoscopic lineation and a more or less complete [010] girdle perpendicular to it. Eclogite specimens with this fabric type were referred to as *L*-type by Helmstaedt *et al.* (1972). Whereas only the omphacite LPO of sample RGM162727 from Engels (1972) (Fig. 7) accords with this pattern (although the author did not mention lineation in his diagrams), three fabrics that in principle might be ascribable to this group were found in this study (EC17, GD3A and GD3B, see Fig. 6). As was the case for *S*-type fabrics, the [010] girdle may contain one or more submaxima of contrasted intensity. *L*-type fabrics have also been reported by Kappel (1967), Kumazawa *et al.* (1971), Van Roermund (1983), Boundy *et al.* (1992) and Godard and Van Roermund (1995). It is emphasized that all intermediates exist between patterns 1 and 2.

Pattern 3, 'annealed fabrics'. These contain a point maximum for $\pi(100)$ perpendicular to the foliation with [001] located in a maxima parallel to *L*. [010] maxima are perpendicular to the lineation and lie in the foliation plane. These fabrics are common in orthopyroxenes from some peridotite massifs and pyroxenites but rare in clinopyroxene (Nicolas and Poirier, 1976; Mainprice and Nicolas, 1989). Philipot and Van Roermund (1992) report for the first time the occurrence of this fabric type in low-temperature eclogites in which grain coarsening processes related to annealing post-dated eclogitic deformation. The omphacite fabric of sample EC17 shown in Fig. 6 is, in some respects, ascribable to this type. Omphacite microstructures in this sample (slightly bulging grain boundaries; Fig. 5c) and its larger grain size in comparison with the other samples (Table 1) also appear to indicate that annealing was operative, although EC17 is an intermediate-temperature (rather than low-temperature) eclogite. Van Roermund (1992) points out that fabrics of this type not related to annealing can only be expected in eclogites metamorphosed at temperatures below 450°C, and that if coarsening processes can be excluded in the formation of these fabrics in medium- and high-temperature eclogites, the LPOs would be indicative of high strain rates.

Pattern 4, 'composite fabrics'. These are characterized by two [010] maxima, one on the foliation plane normal to the lineation and the other perpendicular to the foliation. Both maxima, of either contrasted or similar intensity, can define a pseudo-girdle. These fabrics can be considered as intermediate between either the patterns 1 and 2 described above or between 3 and 1 + 2. Although strictly speaking the only eclogite fabric of this type described in the literature so far is due to Kappel (1967), fabrics exhibiting features of patterns 1 and 2 have been described by Binns (1967) and Godard and Van Roermund (1995). In many respects, most of the fabrics described in this contribution could also be related to this type (Fig. 6). The origin of these fabrics may be related to the combination of the conditions (strain geometry, grain-boundary mobility, mass transfer and strain rate) that produce the other end-member fabric patterns 1, 2 and 3.

Pattern 5, 'misoriented fabrics'. No preferred or weak orientation pattern are shown by LPOs accompanying eclogite granoblastic microstructures. Helmstaedt *et al.* (1972) gave evidence of these fabrics in eclogite xenoliths with mesoscopic granoblastic texture. The $\pi(100)$ omphacite fabrics of most of the samples studied here correspond to this scheme (Fig. 6).

Geometrical relations with the structural XYZ *framework*

As noted in the preceding section, ascription of measured omphacite LPOs to one of the five patterns cited, notably to the 'end-member' patterns 1, 2 and 3, can be misleading. However, their most salient and/or specific features are, ideally, the following: '*S*-type fabrics' (pattern 1) are dominated by [010]-axis maxima normal to the foliation; '*L*-type fabrics' (pattern 2) exhibit dominant [001]-axis maxima parallel to the lineation; and 'annealed fabrics' (pattern 3) are characterized by $\pi(100)$ maxima normal to the foliation. Composite fabrics reflect several of the above features to varying degrees, but are usually closer to one fabric pattern than to the others. Therefore, unambiguous methods of fabric ascription are required.

Stereographic projections give a visual impression of attitude and shape in orientation data distributions that, in turn, can be quantified by means of their eigenvectors (v_1, v_2 and v_3) and eigenvalues (e_1, e_2 and e_3: cf. Scheidegger, 1965; Woodcock, 1977). Routine calculation of these parameters following the procedures outlined by Davis (1973) and Woodcock and Naylor (1983) is facilitated by most popular computer programs for stereographic representation of orientation data (e.g. Allmendinger, 1988; Mancktelow, 1990).

It is suggested here that calculation of the three orthogonal principal axes of a data collection (its eigenvalues and eigenvectors) for each of the [001], [010] and $\pi(100)$ omphacite LPOs could be of great help in that respect. The relative magnitude of the three eigenvalues (e_1, e_2 and e_3, often normalized to sum 1) give a measure of the strength of the fabrics, and orientation of the three eigenvectors relative to *S* and *L* highlights crystallographic fabric symmetry.

Point maximum distributions are characterized by one large and two smaller but similar eigenvalues, whereas girdles exhibit two large and similar eigenvalues and one much smaller. Random fabrics display three similar eigenvalues. Vollmer (1990) proposed utilization of the *P* (point), *G* (girdle) and *R* (random) indices and a

graphical plot of them, which has been followed in Fig. 9. On the basis of these results, the classification of omphacite fabrics from eclogite samples EC2, EC6 and EC9 as '*S*-type fabrics', as well as of those from samples EC17, GD3A and GD3B as '*L*-type fabrics', as presented in Fig. 6, is strengthened.

Eigenvector orientations are given in Fig. 10 for the six samples studied together with the orientations of fabrics produced during D_1 and D_2. This plot illustrates, on one hand, the tendency of v_1 eigenvectors from [001] crystallographic axes in samples with '*L*-type fabrics' to plot close to the lineation, whereas v_1 and v_2 eigenvectors in samples with '*S*-type fabrics' lie within the foliation plane and normal to it defining great circles whose pole is close to the lineation. But on the other hand, and more importantly, eigenvectors plot asymmetrically with respect to the structural *XYZ* reference framework. Asymmetry is consistent between the different samples, and is describable through a 6–8° clockwise rotation about the *Y*-axis of the structural reference.

The external asymmetry of LPOs with respect to rock foliation and lineation are often used to determine shear sense in quartz, calcite, plagioclase, hornblende, orthopyroxene or olivine (Avé Lallemant and Carter, 1970; Gapais and Brun, 1981; Schmid, 1982; Bouchez *et al.*, 1983; Mainprice and Nicolas, 1989). If the conventional interpretation of LPO obliquity is also followed here, this would imply that omphacite LPOs in Cabo Ortegal were produced during deformation along strain paths containing non-coaxial components in addition to any flattening or constriction. The most frequent flow planes would be (010) and the dominant flow direction [001]. The small value of the obliquity angle implies either large values of simple shear (i.e. $\gamma = 7.0$–9.4), or not so large values of simple shear components together with pure shear under general (sub-simple) shear deformation (Means *et al.*, 1980). Rotational strain components imply top-to-the-NNE tectonic displacements, also inferred in the eclogite, the underlying gneiss and the overlying granulite and peridotite, from petrofabrics (Ben Jamaa, 1988), porphyroclast geometry and map relationships (Ábalos *et al.*, 1994).

As regards clinopyroxene in eclogite, asymmetric fabrics have not previously been reported for eclogites in the literature (Godard and Van Roermund, 1995; Passchier and Trouw, 1996). The [001] and [010] fabrics presented by Godard and Van Roermund (1995), considered there as representative of the various coaxial deformation types supposed to occur in eclogites, are roughly symmetrically arranged with respect to the foliation and lineation. Asymmetry in one of the samples is attributed to local changes in foliation and lineation orientations around large garnets. Strong obliquity between omphacite [001]-axes and lineation can be observed in LPOs from eclogitized metagabbros of Boundy *et al.* (1992). Although they are not explicitly

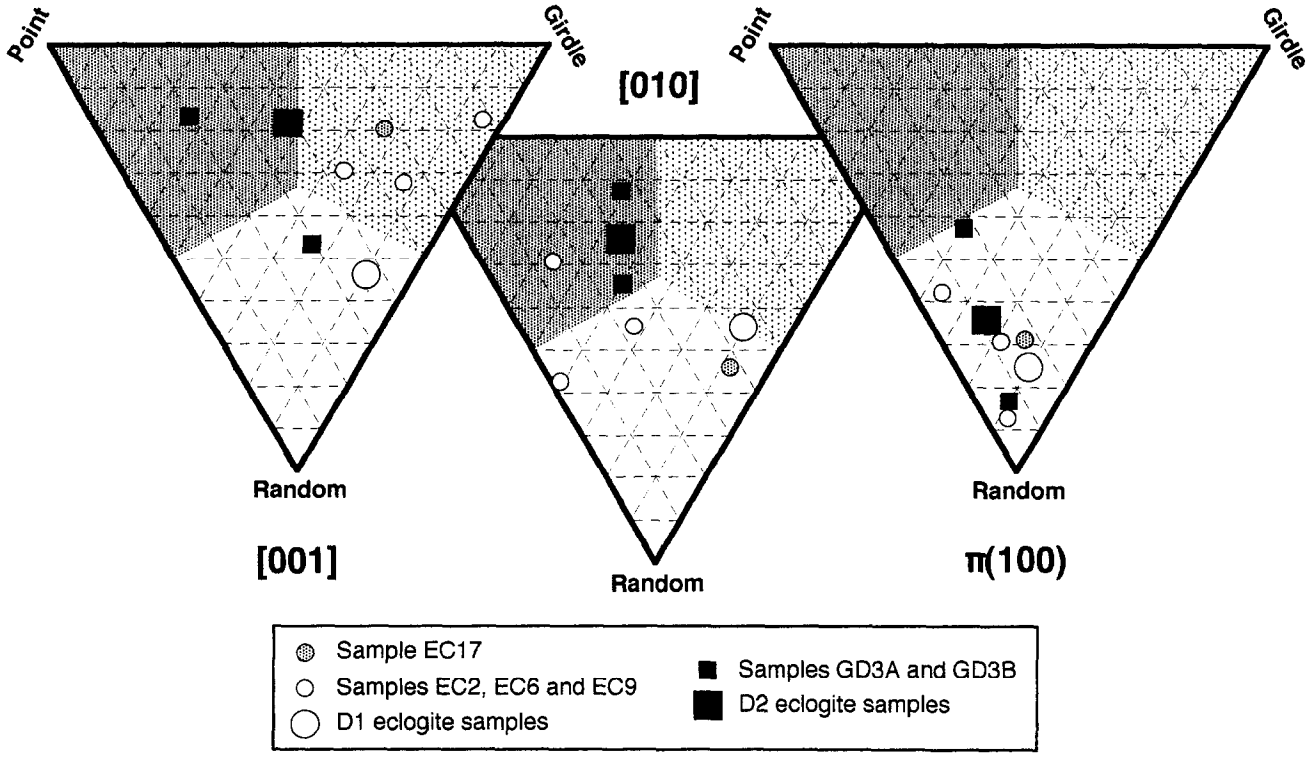

Fig. 9. Triangular fabric diagrams corresponding to omphacite [001]-, [010]- and π(100)-axis orientations based on the indices *P* (point), *G* (girdle) and *R* (random) defined by Vollmer (1990). 'D_1 eclogite samples' and 'D_2 eclogite samples' refer, respectively, to the eigenvalues determined by plotting together the crystallographic axis orientations of samples EC-2, EC-6, EC-9 and EC-17 (500 grains) and those of samples GD3A and GD3B (250 grains).

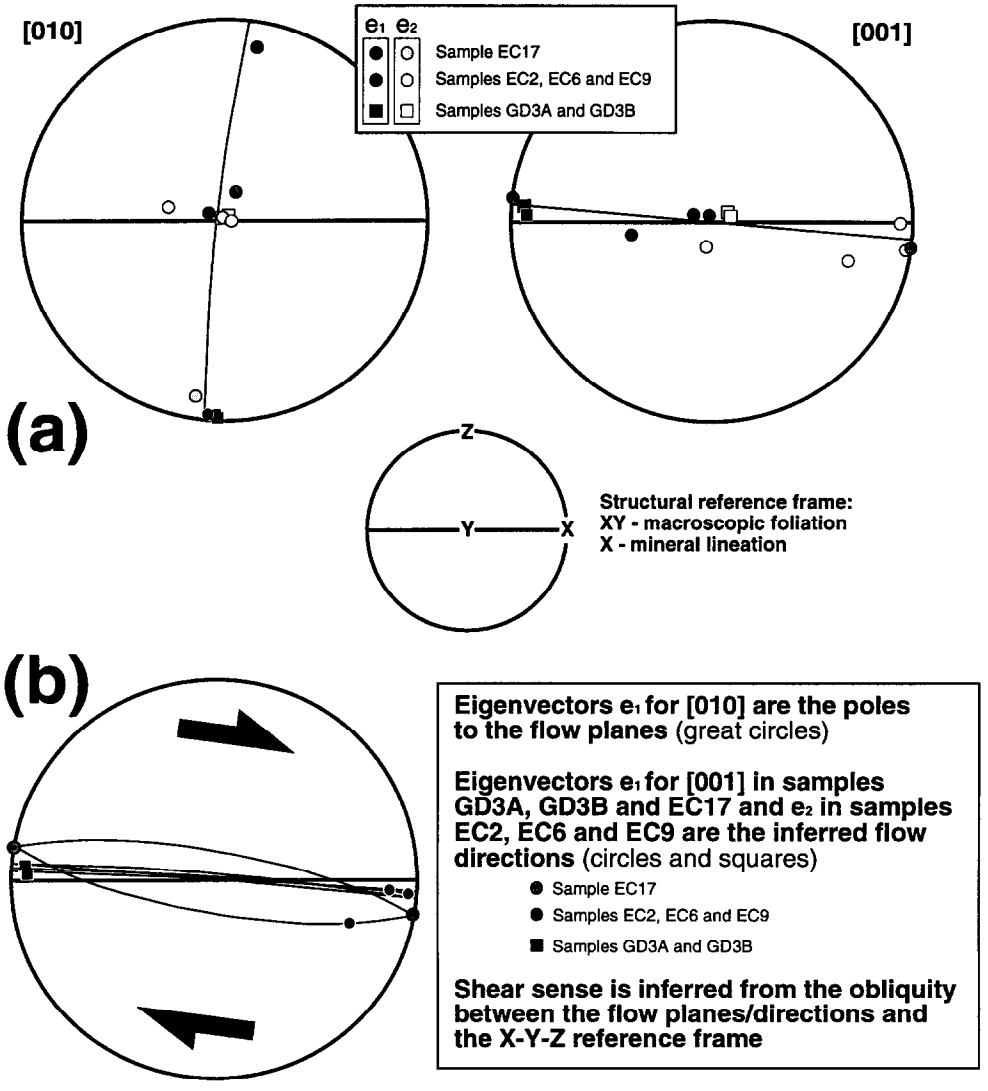

Fig. 10. (a) Stereographic projection (lower-hemisphere) of eigenvector orientations for omphacite [010] and [001] in the samples indicated. (b) Stereographic projection (lower-hemisphere) of orientations from eigenvectors used to infer flow directions (circles and squares) and of the great circles normal to principal [010] eigenvectors, used to infer the flow planes. Note in both cases the obliquity of the great circles (thin lines) with respect to the structural reference framework, which permits inference of the shear sense associated with omphacite crystallographic fabric development. See also text and caption to Fig. 9 for further details.

related to shear-sense kinematic indicators, a consistent geometrical relationship is depicted with the macroscopic structure of the shear zones, with [001]-axis submaxima approximately parallel to the long axes of linear elements contained within shear-zone foliation planes.

DISCUSSION AND CONCLUSIONS

Differences in the fabric patterns in the Cabo Ortegal eclogite massif were attributed to variations in metamorphic grade by Engels (1972). Helmstaedt *et al.* (1972), however, postulated that the effects of pressure and temperature variation with metamorphic grade could be excluded, and that variation in omphacite LPO must be due to contrasting types of deformation. Results of theoretical LPO modelling in quartz using the theory of Taylor–Bishop–Hill (Lister *et al.*, 1978) indicate that LPO development is controlled by the particular combination of crystallographic glide systems active during deformation, the magnitude and symmetry of finite strain, the strain path or kinematic framework, and other deformation parameters such as stress magnitude and strain rate. In the case of eclogite, Godard and Van Roermund (1995) have argued that deformation mechanisms other than dislocation glide should operate during plastic deformation of omphacite.

Crystallographic glide systems active during deformation

The [010]-axis maxima normal to the foliation observed in many omphacite LPOs suggest that (010) is the intracrystalline glide plane, whereas the [001] maxima

within the foliation planes would indicate that this is the intracrystalline flow direction (Nicolas and Poirier, 1976; Nicolas and Christensen, 1987). However, [001](010) has never been identified as a dominant slip system in deformed clinopyroxene. Intracrystalline slip systems recognized from experimental deformation of diopside (Kirby and Christie, 1977; Avé Lallemant, 1978; Kollé and Blacic, 1982; Kirby and Kronenberg, 1984; Boland and Tullis, 1986; Ingrin *et al.*, 1991, 1992; Raterron and Jaoul, 1991; Raterron *et al.*, 1994) occur in naturally deformed omphacite (Lorimer *et al.*, 1972, Champness *et al.*, 1974; Van Roermund and Boland, 1981; Van Roermund, 1984, 1992; Buatier *et al.*, 1991; Van Roermund and Lardeaux, 1991). The operating slip systems inferred from TEM observations of eclogites metamorphosed under conditions of *ca* 700°C and 1.5 GPa are $1/2<110>\{110\}$, [001]{110} and [001](100), assisted by dislocation climb. The intracrystalline slip systems [001](100) and [001]{110} accommodate shear parallel to the lineation and dominate over $1/2<110>\{110\}$. The latter slip system, since it is oriented to accommodate shortening normal to the foliation, thereby facilitates rotation of the [100]- and [010]-axes in a girdle perpendicular to lineation (Buatier *et al.*, 1991). Godard and Van Roermund (1995) conclude that to explain the LPOs of omphacite, similar to those described here, it is also necessary to invoke mass transfer and competitive growth processes.

Symmetry of finite strain and the kinematic framework

As proposed by Godard and Van Roermund (1995), the resemblance of the eclogite fabric types to *L–S* tectonites suggests that omphacite 'constriction fabrics' (the *L*-type of Helmstaedt *et al.*, 1972) are compatible with recrystallization under conditions of constriction causing the linear alignment of clinopyroxene, whereas 'flattening fabrics' (the *S*-type of Helmstaedt *et al.*, 1972) may indicate recrystallization during flattening leading to foliation development, and that gradations between these two patterns should be present. These proposals are exemplified by the eclogite fabrics (microtextures and LPOs) of Cabo Ortegal, as shown above.

Godard and Van Roermund (1995) point out that omphacite LPOs from Cabo Ortegal remain constant over the entire eclogite belt, based upon Engels' (1972) work. They noted as well that strain partitioning could have taken place between eclogites and the surrounding rocks. Omphacite LPOs in the eclogites could be indicative of some kind of coaxial deformation, whereas the strain symmetry in the surrounding rocks is predominantly non-coaxial. Partitioning of deformation between the eclogite and the neighbouring rocks, within the eclogite stack, and the occurrence of non-coaxial strain components have been shown by Ábalos *et al.* (1994, 1996) on the basis of porphyroclast geometry and the reconstructed architecture of the eclogite stack (Fig. 3). The omphacite LPO obliquity with respect to foliation and lineation detected here also supports this conclusion, thereby implying that the eclogite ductile deformation includes non-coaxial strain components additional to any flattening or constriction strain paths. In addition, rotational strain components in the eclogite LPOs are congruent with top-to-the-NNE tectonic displacements also inferred in the neighbouring high-pressure granulite and gneiss from independent shear-sense criteria.

Stress magnitude and strain rate

The dislocation substructure of the Cabo Ortegal 'Gal' sample studied by Godard and Van Roermund (1995) was produced by dislocation creep and climb during plastic deformation. Climb processes are highly influenced by temperature and strain rate. Although diopside may not be a good analogue for omphacite, Godard and Van Roermund (1995) found that extrapolated creep laws (e.g. Avé Lallemant, 1978) for eclogite clinopyroxene at temperatures below 700°C would require unreasonably high stress and/or low strain rates to accommodate strain by dislocation creep.

Growth of omphacite neoblasts during dynamic recrystallization has been suggested by Champness *et al.* (1974), Buatier *et al.* (1991) and Philipot and Van Roermund (1992), and was observed during experimental deformation of polycrystalline diopside by Carter *et al.* (1972) at 1000–1200°C concomitant with LPO development. Boland and Tullis (1986) also showed that deformation and grain-boundary mobility are facilitated by the addition of water. The clinopyroxene fabrics shown in Figs 6–8 indicate that temperatures of deformation were of high-grade metamorphism, $\geq$825°C according to Estey and Douglas (1986).

Although applying paleopiezometers to clinopyroxene is hampered by the lack of experimental verification, use of the empirical law (for diopside at 1200°C) of Avé Lallemant (1978) to determine the flow stress from dynamically recrystallized omphacite neoblast size yields very low differential stresses between 4 and 10 MPa for the 'massive eclogite', and between 15 and 20 MPa for the 'deformed eclogite'.

The results obtained by Ábalos *et al.* (1996) for quartz vein (within eclogite) ductile deformation are in agreement with those reported above and permit the comparison of the conceivable minimum flow stress and strain rate undergone by the Cabo Ortegal eclogite. Ductile deformation of the 'deformed eclogite' during D_1 (possibly under hydrous conditions) would have taken place under confining pressures of 1.5–1.7 GPa, temperatures well above 600°C, low paleopiezometrically calculated differential stress (10 MPa) and slow strain rates (10^{-17}–10^{-15} s^{-1}). Later localized deformation of the 'deformed eclogite' during D_2 would have occurred under temperatures down to 520°C related to higher differential stress ($\geq$25 MPa) and faster strain rates (between 10^{-14} and 10^{-12} s^{-1}). Although the state of stress in the deeper levels of the crust and subduction realms is poorly

constrained and obscure in the literature, another example where microstructures indicate a very low magnitude of differential stress (1–2 MPa at 600°C) during high-pressure metamorphism (at depths of burial of 70–80 km) comes from the Tauern Window in the Eastern Alps (Stöckhert *et al.*, 1995).

Thermomechanical and kinematic significance of omphacite mineral lineation

Regionally widespread mineral and/or stretching lineations within a tectonic foliation are used as fundamental data for kinematic syntheses because they may furnish information on the direction of tectonic transport ('*a*' lineations of Turner and Weiss, 1963; e.g. Shackleton and Ries, 1984; Burg *et al.*, 1987; Ildefonse *et al.*, 1990). Foundations to this are the facts that: (1) tectonic foliations approximately trace the *XY* plane of tectonic strain; whereas (2) stretching lineations contained in a continuous foliation trace the *X* direction of strain related to the deformation phase in which they developed; and (3) a foliation defined by parallel minerals that show a growth fabric without signs of post-crystalline deformation must have formed under metamorphic conditions during which these minerals were stable (Passchier and Trouw, 1996).

All the results presented above bear on the kinematic and mechanical significance of the NNE-trending mineral and stretching lineations and the associated top-to-the-NNE sense of movement of hangingwall blocks in the Cabo Ortegal eclogite. Lineation is defined in the eclogite by shape-preferred orientation of omphacite and other minerals which are stable under high-pressure metamorphic conditions estimated through thermobarometry. This structure is associated with strong omphacite LPOs formed by crystal-plastic processes operative under high-grade temperatures, and is parallel and kinematically comparable on a regional basis to the mineral and stretching lineations of neighbouring high-pressure metaperidotites, granulites and gneisses of the Cabo Ortegal complex. Non-coaxial strain regimes and contrasting strain paths may be inferred from asymmetry of LPOs with respect to the structural framework provided by foliation and lineation and from LPO variations, respectively.

The early deformation phases of many collisional orogens are characterized by regionally consistent stretching lineations subparallel to the orogen and to associated isoclinal and sheath folds (Ellis and Watkinson, 1987). These authors, based on kinematic modelling of modern oblique convergent margins, suggest that only such early structures reflect the relative plate motions. It is proposed here that the tectonic foliations and mineral/stretching lineations studied in Cabo Ortegal are consistent with shear-zone deformation under eclogite-facies conditions in a deep subduction realm, and reflect tectonic amalgamation related to the eo-Hercynian NNE-directed oblique collision and emplacement of a lithospheric mantle wedge.

Acknowledgements—Sample EC17 was kindly provided by J. I. Gil Ibarguchi. I thank G. Godard and D. Shelley for very helpful and constructive reviews of the manuscript. R. J. Norris is thanked for his careful correction of the odd English and the editorial handling. This study was financially supported by the Spanish D.G.I.C.Y.T. PB95/1035 grant.

REFERENCES

Ábalos, B., Mendía, M. S. and Gil Ibarguchi, J. I. (1994) Structure of the Cabo Ortegal Eclogite-Facies Zone (NW Iberia). *Comptes Rendus de l'Académie des Sciences, Paris (Série 2)* **319**, 1231–1238.

Ábalos, B., Gil Ibarguchi, J. I., Mendía, M. S. and Azcárraga, J. (1995) High-pressure strain in eclogites: evidence from garnet-aggregate image analysis and clinopyroxene crystallographic fabric studies. *Bochumer Geologische und Geotechnik Arbeiten* **44**, 1–4.

Ábalos, B., Azcárraga, J., Gil Ibarguchi, J. I., Mendía, M. S. and Santos Zalduegui, J. F. (1996) Flow stress, strain rate and effective viscosity evaluation in a high-pressure nappe (Cabo Ortegal, Spain). *Journal of Metamorphic Geology* **14**, 227–248.

Allmendinger, R. W. (1988) *STEREONET; A Plotting Program for Orientation Data.* Computer program and manual.

Arenas, R., Gil Ibarguchi, I., González Lodeiro, F., Klein, E., Martínez Catalán, J. R., Ortega Gironés, E., de Pablo Maciá, J. G. and Peinado, M. (1986) Tectono-stratigraphic units in the complexes with mafic and related rocks of the NW of the Iberian Massif. *Hercynica* **2**, 87–110.

Avé Lallemant, H. G. (1978) Experimental deformation of diopside and websterite. *Tectonophysics* **48**, 1–27.

Avé Lallemant, H. G. and Carter, N. (1970) Syntectonic recrystallization of olivine and modes of flow in the upper mantle. *Bulletin of the Geological Society of America* **81**, 2203–2220.

Baker, D. W. and Carter, N. L. (1972) Seismic velocity anisotropy calculated for ultramafic minerals and aggregates. In *Flow and Fracture of Rocks. The Griggs Volume*, eds H. C. Heard, I. Y. Borg, N. L. Carter and C. B. Raleigh, pp. 157–166. American Geophysical Union, Geophysical Monograph **16**.

Banno, S. and Yoshino, G. (1965) Eclogite-bearing peridotite mass at Higasiakaisi-Yama in the Bessi area, central Sikoku, Japan. In *Upper Mantle Symposium*, ed. H. E. Smith and T. Sorgenfrei, pp. 150–160. I.U.G.S., Copenhagen.

Ben Jamaa, N. (1988) Les peridotites de Bay of Islands (Terre Neuve) et de Cap Ortegal (Espagne): approche petro-structurale. Unpublished thesis, University of Paris VII.

Bernard-Griffiths, J., Peucat, J. J., Cornichet, J., Iglesias Ponce de León, M. and Gil Ibarguchi, J. I. (1985) U–Pb, Nd isotope and REE geochemistry in eclogites from the Cabo Ortegal Complex, Galicia, Spain: an example of REE inmobility conserving MORB-like patterns during high-grade metamorphism. *Chemical Geology* **52**, 217–225.

Binns, R. A. (1967) Barroisite-bearing eclogite from Naustdal, Sogn og Fjordane, Norway. *Journal of Petrology* **8**, 349–371.

Boland, J. N. and Tullis, T. E. (1986) Deformation behavior of wet and dry clinopyroxenite in the brittle to ductile transition region. In *Mineral and Rock Deformation: Laboratory Studies. The Paterson Volume*, eds B. E. Hobbs and H. C. Heard, pp. 35–49. American Geophysical Union, Geophysical Monograph **36**.

Bouchez, J. L., Lister, G. S. and Nicolas, A. (1983) Fabric asymmetry and shear sense in movement zones. *Geologische Rundschau* **72**, 401–419.

Boundy, T. M., Fountain, D. M. and Austrheim, H. (1992) Structural development and petrofabrics of eclogite facies shear zones, Bergen Arcs, western Norway: implications for deep crustal deformational processes. *Journal of Metamorphic Geology* **10**, 127–146.

Buatier, M., Van Roermund, H. L. M., Drury, M. R. and Lardeaux, J. M. (1991) Deformation and recrystallization mechanisms in naturally deformed omphacites from the Sesia-Lanzo zone: geophysical consequences. *Tectonophysics* **195**, 11–27.

Burg, J. P., Balé, P., Brun, J. P. and Girardeau, J. (1987) Stretching lineations and transport direction in the Ibero-Armorican Arc during the Siluro-Devonian collision. *Geodynamica Acta* **1**, 71–81.

Carswell, D. A. (1990) Eclogites and the eclogite facies: definitions and classification. In *Eclogite Facies Rocks*, ed. D. A. Carswell, pp. 1–13. Blackie, New York.

Carter, N. L., Baker, D. W. and George, R. P. (1972) Seismic anisotropy, flow, and constitution of the upper mantle. Seismic velocity anisotropy calculated for ultramafic minerals and aggregates. In *Flow and Fracture of Rocks. The Griggs Volume*, eds H. C. Heard, I. Y. Borg, N. L. Carter and C. B. Raleigh, pp. 167–179. American Geophysical Union, Geophysical Monograph **16**.

Champness, P. E., Fyfe, W. S. and Lorimer, G. W. (1974) Dislocations and voids in pyroxene from a low-temperature eclogite: mechanisms of eclogite formation. *Contributions to Mineralogy and Petrology* **43**, 91–98.

Davis, J. C. (1973) *Statistics and Data Analysis in Geology*. Wiley, New York.

Ellis, M. A. and Watkinson, A. J. (1987) Orogen-parallel extension and oblique tectonics: the relation between stretching lineations and relative plate motions. *Geology* **15**, 1022–1025.

Engels, J. P. (1972) The catazonal poly-metamorphic rocks of Cabo Ortegal (NW Spain), a structural and petrographic study. *Leidse Geologische Mededelingen* **48**, 83–133.

Eskola, P. (1921) On the eclogites of Norway. *Vidensk.-Selsk. Skr. I. Mat. Naturv. Kl.* **8**, 1–118.

Estey, L. H. and Douglas, B. J. (1986) Upper mantle anisotropy: a preliminary model. *Journal of Geophysical Research* **91**, 11393–11406.

Flinn, D. (1962) On folding during three-dimensional progressive deformation. *Quarterly Journal of the Geological Society of London* **118**, 385–428.

Gapais, D. and Brun, J. P. (1981) A comparison of mineral grain fabrics and finite strain in amphibolites from eastern Finland. *Canadian Journal of Earth Sciences* **18**, 995–1003.

Gil Ibarguchi, I., Ábalos, B., Campillo, A., Higuero, A., López, B., Pinilla, V., Rodriguez, C., Rodriguez, R. and Urtiaga, K. (1987) Asociaciones con granate-clinopiroxeno en la unidad catazonal superior del complejo de Cabo Ortegal. *Cuadernos del Laboratorio Geológico de Laxe* **12**, 165–181.

Gil Ibarguchi, J. I., Mendia, M., Girardeau, J. and Peucat, J. J. (1990) Petrology of eclogites and clinopyroxene–garnet metabasites from the Cabo Ortegal Complex (northwestern Spain). *Lithos* **25**, 133–162.

Girardeau, J., Gil Ibarguchi, J. I. and Ben Jamaa, N. (1989) Evidence for a heterogeneous upper mantle in the Cabo Ortegal Complex, Spain. *Science* **245**, 1231–1233.

Godard, G. (1988) Petrology of some eclogites in the Hercynides: the eclogites from the southern Armorican massif, France. In *Eclogites and Eclogite-facies Rocks. Developments in Petrology*, ed. D. C. Smith, Vol. 12, pp. 451–519. Elsevier, Amsterdam.

Godard, G. and Van Roermund, H. L. M. (1995) Deformation-induced clinopyroxene fabrics from eclogites. *Journal of Structural Geology* **17**, 1425–1443.

Helmstaedt, H., Anderson, D. L. and Gavasci, A. T. (1972) Petrofabric studies of eclogite, spinel websterite, and spinel-lherzolite xenoliths from kimberlite-bearing breccia pipes in southeastern Utah and northeastern Arizona. *Journal of Geophysical Research* **77**, 4350–4365.

Ildefonse, B., Lardeaux, J. M. and Caron, J. M. (1990) The behavior of shape preferred orientations in metamorphic rocks: amphiboles and jadeites from the Monte Mucrone area (Sesia-Lanzo Zone, Italian Western Alps). *Journal of Structural Geology* **12**, 1005–1011.

Ingrin, J., Doukhan, N. and Doukhan, J. C. (1991) High-temperature deformation of diopside single crystal—2. Transmission electron microscopy investigation of the defect microstructures. *Journal of Geophysical Research* **96**, 14287–14297.

Ingrin, J., Doukhan, N. and Doukhan, J. C. (1992) Dislocation glide systems in diopside single crystals deformed at 800–900°C. *European Journal of Mineralogy* **4**, 1291–1302.

Kappel, F. (1967) Die Eklogite meidling im Tal und Mitterbachgraben im Niederösterreichischen Moldanubicum südlich der Donau. *Neues Jahrbuch Mineralogie Abhandungen* **107**, 266–298.

Kirby, S. H. and Christie, J. M. (1977) Mechanical twinning in diopside $Ca(Mg,Fe)Si_2O_6$: structural mechanism and associated crystal defects. *Physics and Chemistry of Minerals* **1**, 137–163.

Kirby, S. H. and Kronenberg, A. K. (1984) Deformation of clinopyroxenite: evidence for a transition in flow mechanisms and semibrittle behavior. *Journal of Geophysical Research* **89**, 3177–3192.

Kollé, J. J. and Blacic, J. D. (1982) Deformation of single-crystal clinopyroxenes: 1. Mechanical twinning in diopside and hedenbergite. *Journal of Geophysical Research* **87**, 4019–4034.

Kozlowski, K. (1965) The granulitic complex of Stary Gieraltow, East Sudetes. *Archiwumm Mineralogiczne* **25**, 5–123.

Kumazawa, M., Helmstaedt, H. and Masaki, K. (1971) Elastic properties of eclogite xenoliths from diatremes of the East Colorado Plateau and their implications for the upper mantle structure. *Journal of Geophysical Research* **76**, 1231–1247.

Lister, G. S., Paterson, M. S. and Hobbs, B. E. (1978) The simulation of fabric development in plastic deformation and its application to quartzites: the model. *Tectonophysics* **45**, 107–158.

Lorimer, G. W., Champness, P. E. and Spooner, E. T. C. (1972) Dislocation distributions in naturally deformed omphacite and albite. *Nature, Physical Sciences* **239**, 108–109.

Mainprice, D. and Nicolas, A. (1989) Development of shape and lattice preferred orientations: application to the seismic anisotropy of the lower crust. *Journal of Structural Geology* **11**, 175–189.

Mancktelow, N. S. (1990) *STEREOPLOT*. Computer program plus user's guide and reference manual.

Means, W. D., Hobbs, B. E., Lister, G. and Williams, P. F. (1980) Vorticity and non-coaxiality in progressive deformations. *Journal of Structural Geology* **2**, 371–378.

Nicolas, A. and Christensen, N. I. (1987) Formation of anisotropy in upper mantle peridotites–a review. In *Composition, Structure and Dynamics of the Lithosphere–Astenosphere System*, eds K. Fuchs and C. Froidevaux, pp. 111–123. American Geophysical Union, Geodynamics Series **16**.

Nicolas, A. and Poirier, J. P. (1976) *Crystalline Plasticity and Solid-state Flow in Metamorphic Rocks*. Wiley, New York.

Passchier, C. W. and Trouw, R. A. J. (1996) *Microtectonics*. Springer, Berlin.

Peucat, J. J., Bernard-Griffiths, J., Gil Ibarguchi, J. I., Dallmeyer, R. D., Menot, R. P., Cornichet, J. and Iglesias Ponce de León, M. (1990) Geochemical and geochronological cross section of the deep variscan crust: the Cabo Ortegal high-pressure nappe (NW Spain). In *Terranes in the Variscan Belt of Europe and Circum-Atlantic Paleozoic Orogens*, ed. Ph. Matte. *Tectonophysics* **177**, 263–292.

Philipot, P. and Van Roermund, H. L. M. (1992) Deformation processes in eclogitic rocks: evidence for the rheological delamination of the oceanic crust in deeper levels of subduction zones. *Journal of Structural Geology* **14**, 1059–1077.

Raterron, P. and Jaoul, O. (1991) High-temperature deformation of diopside single crystal—1. Mechanical data. *Journal of Geophysical Research* **96**, 14277–14286.

Raterron, P., Doukhan, N., Jaoul, O. and Doukhan, J. C. (1994) High-temperature deformation of diopside IV: predominance of {110} glide above 1000°C. *Physics of Earth and Planetary Interiors* **82**, 209–222.

Santos Zalduegui, J. F. (1994) Geocronología y geoquímica isotópica de diferentes unidades de los complejos alóctonos de Cabo Ortegal y Malpica-Tuy (NO de España). Ph.D. thesis, University País Vasco, Bilbao.

Scheidegger, A. E. (1965) On the statistics of the orientation of bedding planes, grain axes and similar sedimentological data. *U.S. Geological Survey Professional Paper* **525-C**, C164–C167.

Schmid, S. M. (1982) Microfabric studies as indicators of deformation mechanisms and flow laws operative in mountain building. In *Mountain Building Processes*, ed. K. J. Hsu, pp. 95–110. Academic Press, London.

Schreyer, W. (1995) Ultradeep metamorphic rocks: the retrospective viewpoint. *Journal of Geophysical Research* **100**, 8353–8366.

Shackleton, R. M. and Ries, A. (1984) The relation between consistent stretching lineations and plate motions. *Journal of Structural Geology* **6**, 111–117.

Smulikowski, K. (1964) An attempt at eclogite classification. *Bull. Acad. Pol. Sci., Ser. Géol. et Géograph.* **13**, 11–18.

Stöckhert, B., Nowlan, E. V. and Massone, H.-J. (1995) High-pressure metamorphism under low differential stress—the microstructural record of a metapelite from the eclogite zone, Tauern Window, Eastern Alps. *Bochumer Geologische und Geotechnik Arbeiten* **44**, 229–234.

Turner, F. J. and Weiss, L. E. (1963) *Structural Analysis of Metamorphic Tectonites*. McGraw-Hill, New York.

Van Roermund, H. L. M. (1983) Petrofabrics and microstructures of omphacites in a high temperature eclogite from the Swedish Caledonides. *Bulletin de Minéralogie* **106**, 709–713.

Van Roermund, H. L. M. (1984) Omphacite microstructures from a Spanish eclogite. *Textures and Microstructures* **6**, 105–116.

Van Roermund, H. L. M. (1992) Thermal and deformation induced omphacite microstructures from eclogites; implications for the formation and uplift of HP metamorphic terrains. *Trends in Mineralogy* **1**, 117–151.

Van Roermund, H. L. M. and Boland, J. N. (1981) The dislocation substructures of naturally deformed omphacites. *Tectonophysics* **78**, 403–418.

Van Roermund, H. L. M. and Lardeaux, J. M. (1991) Modification of omphacite domain sizes in omphacite by dislocation glide and creep mechanisms and its petrological consequences. *Mineralogical Magazine* **55**, 397–407.

Vogel, D. E. (1967) Petrology of eclogite- and pyrigarnite-bearing polymetamorphic rock complex at Cabo Ortegal, NW Spain. *Leidse Geologische Mededelingen* **40**, 121–213.

Vollmer, F. W. (1990) An application of eigenvalue methods to structural domain analysis. *Bulletin of the Geological Society of America* **102**, 786–791.

Woodcock, N. H. (1977) Signification of fabric shapes using an eigenvalue method. *Bulletin of the Geological Society of America* **88**, 1231–1236.

Woodcock, N. H. and Naylor, M. A. (1983) Randomness testing in three-dimensional orientation data. *Journal of Structural Geology* **5**, 539–548.

Yoshino, G. (1961) Structural–petrological studies of peridotite and associated rocks of the Higashiakaishi-yama district, Shikoku, Japan. *Journal of Science Hiroshima University Series C* **3**, 343–402.

Yoshino, G. (1964) Ultrabasic mass in the Higashiakaishi-yama district, Shikoku, southern Japan. *Journal of Science Hiroshima University Series C* **4**, 333–364.